

## KLOE extraction of $a_\mu^{\pi\pi}$ in the mass range [0.35, 0.95] GeV<sup>2</sup>

The KLOE Collaboration

F. Ambrosino, A. Antonelli, M. Antonelli, F. Archilli, C. Bacci, P. Beltrame, G. Bencivenni, S. Bertolucci, C. Bini, C. Bloise, S. Bocchetta, V. Bocci, F. Bossi, P. Branchini, R. Caloi, P. Campana, G. Capon, T. Capussela, F. Ceradini, S. Chi, G. Chiefari, P. Ciambrone, E. De Lucia, A. De Santis, P. De Simone, G. De Zorzi, A. Denig, A. Di Domenico, C. Di Donato, S. Di Falco, B. Di Micco, A. Doria, M. Dreucci, G. Felici, A. Ferrari, M. L. Ferrer, G. Finocchiaro, S. Fiore, C. Forti, P. Franzini, C. Gatti, P. Gauzzi, S. Giovannella, E. Gorini, E. Graziani, M. Incagli, W. Kluge, V. Kulikov, F. Lacava, G. Lanfranchi, J. Lee-Franzini, D. Leone, M. Martini, P. Massarotti, W. Mei, L. Meola, S. Miscetti, M. Moulson, S. Müller, F. Murtas, M. Napolitano, F. Nguyen, M. Palutan, E. Pasqualucci, A. Passeri, V. Patera, F. Perfetto, M. Primavera, P. Santangelo, G. Saracino, B. Sciascia, A. Sciubba, F. Scuri, I. Sfiligoi, T. Spadaro, M. Testa, L. Tortora, P. Valente, B. Valeriani, G. Venanzoni, R. Versaci, G. Xu

The KLOE Experiment at the  $\phi$  factory DAΦNE has measured the cross section  $\sigma(e^+e^- \rightarrow \pi^+\pi^-\gamma)$  using two different selection schemes: requiring the photon emission at small polar angle and detecting the photon at large polar angle in the calorimeter. Using a theoretical radiator function we extract the pion form factor and obtain the  $\pi\pi$  contribution to the anomalous magnetic moment of the muon. Results presented here come from the analysis of 240 pb<sup>-1</sup> collected in 2002, with improved systematic uncertainty with respect to the published KLOE analysis. We also include an update of the previous analysis.

### I. INTRODUCTION

The muon magnetic anomaly is one of the best known quantities in Particle Physics. Recent measurements performed at Brookhaven, reach an accuracy of 0.54 ppm [1]. Theorists derive a number that differs from the experimental value by 3.2 standard deviations [2]. The main source of uncertainty of the theoretical estimate stems from the hadronic contributions, not calculable within the perturbative regime of QCD. The hadronic contribution at the lowest order,  $a_\mu^{hlo}$ , is obtained from a dispersion integral of hadronic cross section measurements. Incidentally, the annihilation reaction with the final state  $\pi^+\pi^-$  accounts for  $\sim 70\%$  of  $a_\mu^{hlo}$  and  $\sim 60\%$  of the uncertainty.

### II. DAΦNE AND KLOE

DAΦNE is an  $e^+e^-$  collider running at  $\sqrt{s} \simeq M_\phi$ , the  $\phi$  meson mass, which has provided an integrated luminosity of about 2.5 fb<sup>-1</sup> to the KLOE experiment up to year 2006. In addition, about 250 pb<sup>-1</sup> of data have been collected at  $\sqrt{s} \simeq 1$  GeV, in 2006.

Present results are based on 240 pb<sup>-1</sup> of data taken in 2002, sufficient to reach a statistical relative error less than 0.2% in the  $\pi\pi$  contribution on the muon magnetic anomaly,  $a_\mu^{\pi\pi}$ .

The KLOE detector consists of a drift chamber [3] with excellent momentum resolution ( $\sigma_p/p \sim 0.4\%$  for tracks with polar angle larger than 45°) and an electromagnetic calorimeter [4] with good energy ( $\sigma_E/E \sim 5.7\%/\sqrt{E}$  [GeV]) and precise time ( $\sigma_t \sim 54$  ps/ $\sqrt{E}$  [GeV]  $\oplus$  50 ps) resolution.

### III. MEASUREMENT OF THE $\sigma_{\pi\pi}$ CROSS SECTION

At DAΦNE, we measure the differential spectrum of the  $\pi^+\pi^-$  invariant mass,  $M_{\pi\pi}$ , from Initial State Radiation (ISR) events,  $e^+e^- \rightarrow \pi^+\pi^-\gamma$ , and extract the total cross section  $\sigma_{\pi\pi} \equiv \sigma_{e^+e^- \rightarrow \pi^+\pi^-}$  using the following formula [5]:

$$M_{\pi\pi}^2 \frac{d\sigma_{\pi\pi\gamma}}{dM_{\pi\pi}^2} = \sigma_{\pi\pi}(M_{\pi\pi}^2) H(M_{\pi\pi}^2), \quad (1)$$

where  $H$  is the radiator function. This formula neglects Final State Radiation (FSR) terms.

#### A. Small angle $\gamma$ selection, SA

The cross section for ISR photons has a pronounced divergence in the forward angle (relative to the beam direction), then overwhelmingly dominates over FSR photon production. Thus, the fiducial volume of the SA event selection scheme, both for the published 2001 [6] and 2002 data are based on the following selection criteria:

- a) two tracks with opposite charge within the polar angle range  $50^\circ < \theta < 130^\circ$ , this helps in obtaining good reconstructed tracks;
- b) small angle photon,  $\theta_\gamma < 15^\circ$  ( $\theta_\gamma > 165^\circ$ ), the photon is not explicitly detected and its direction is reconstructed from the track momenta,  $\vec{p}_\gamma = -(\vec{p}_{\pi^+} + \vec{p}_{\pi^-})$ , this enhances the probability that it is an ISR photon.

This fiducial volume implies the following advantages:

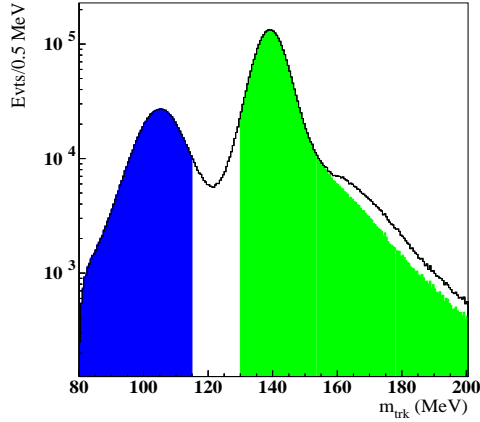


FIG. 1: Discrimination of the  $\mu^+\mu^-\gamma$  (filled dark histogram) from the  $\pi^+\pi^-\gamma$  (filled light histogram) events, after the selection discussed in the text. The residual contamination of  $\pi^+\pi^-\pi^0$  events is evident at high  $m_{trk}$  values.

- FSR at the Leading Order is reduced to the 0.3% level;
- the contamination from the resonant process  $e^+e^- \rightarrow \phi \rightarrow \pi^+\pi^-\pi^0$  – where at least one of photons coming from the  $\pi^0$  is lost – is reduced to the level of  $\sim 5\%$ .

Discrimination of  $\pi^+\pi^-\gamma$  from  $e^+e^- \rightarrow e^+e^-\gamma$  events is done via particle identification [7] based on the time of flight, on the shape and the energy of the clusters associated to the tracks. In particular, electrons deposit most of their energy in the first planes of the calorimeter while minimum ionizing muons and pions release uniformly the same energy in each plane. An event is selected if at least one of the two tracks has not being identified as an electron. This criterion results in a rejection power of 97% for  $e^+e^-\gamma$  events, while retaining a selection efficiency of  $\sim 100\%$  for  $\pi^+\pi^-\gamma$  events.

Contaminations from the processes  $e^+e^- \rightarrow \mu^+\mu^-\gamma$  and  $\phi \rightarrow \pi^+\pi^-\pi^0$  are rejected by cuts on the track mass variable,  $m_{trk}$ , defined by the four-momentum conservation – assuming a final state consisting of two particles with the same mass and one photon – and on the missing mass,  $m_{miss} = \sqrt{E_X^2 - |\vec{P}_X|^2}$ , defined assuming the process is  $e^+e^- \rightarrow \pi^+\pi^-X$ . Fig. 1 shows the separation between  $\pi^+\pi^-\gamma$  and  $\mu^+\mu^-\gamma$  events, achieved selecting different  $m_{trk}$  regions around the mass peaks.

Nevertheless, the small  $\gamma$  angle selection does not allow us to cover the threshold region, where the photon takes the maximum available momentum and the pions recoil the opposite direction with minimum opening angle.

## B. Large angle $\gamma$ selection, LA

The threshold region becomes accessible as the photon is emitted into the same solid angle of the pion tracks. Thus, a different KLOE analysis is done requiring the detection of at least one photon of energy larger than 50 MeV and  $50^\circ < \theta_\gamma < 130^\circ$  in the calorimeter. This allows the closure of the kinematics with the following variables:

- the angle between the photon direction and the missing momentum,  $\vec{p}_{miss} = -(\vec{p}_{\pi^+} + \vec{p}_{\pi^-})$ ;
- the  $\chi^2$  of a kinematic fit implementing four-momentum conservation and  $\pi^0$  mass as constraints.

These requirements are applied to reject the  $\pi^+\pi^-\pi^0$  contamination – much larger than in the SA requirement. Moreover, this LA selection is sensitive to larger FSR effects, including interference from the resonant [10] decays  $\phi \rightarrow f_0(980)\gamma$ , with  $f_0(980) \rightarrow \pi^+\pi^-$  and  $\phi \rightarrow \rho^\pm\pi^\mp$ , with  $\rho^\pm \rightarrow \pi^\pm\gamma$ . The phases and couplings of these interference effects have to be obtained from Monte Carlo using phenomenological models [11, 12].

## C. Improvements with respect to the published analysis

The analysis of data taken since 2002 benefits from cleaner and more stable running conditions of DAΦNE resulting in less machine background. In particular the following changes are applied with respect to the data taken in 2001:

- an additional trigger level was implemented at the end of 2001 to eliminate a 30% loss due to pions penetrating up to the outer calorimeter plane and being misidentified as cosmic rays events (from 2002 on, this inefficiency has decreased down to 0.2% on  $\pi^+\pi^-\gamma$  events);
- the offline background filter, which contributed the largest experimental systematic uncertainty to the published work [6], has been improved and includes now a downscale algorithm providing an unbiased control sample. This greatly facilitates the evaluation of the filter efficiency which increased from 95% to 98.5%, with negligible systematic uncertainty.

In addition to the aforementioned items, the knowledge of the detector response and of the KLOE simulation program has been improved.

#### IV. LUMINOSITY

The absolute normalization of the data sample is measured using large angle Bhabha scattering events,  $55^\circ < \theta < 125^\circ$ , with a cross section  $\sigma \simeq 430$  nb. The integrated luminosity,  $\mathcal{L}$ , is provided [13] dividing the observed number of these events by the effective cross section evaluated by the Monte Carlo generator **Babayaga** [14], including QED radiative corrections with the parton shower algorithm, inserted in the code simulating the KLOE detector. Recently, an updated version of the generator, **Babayaga@NLO** [15], has been released. The new predicted cross section decreased

systematic errors on $\mathcal{L}$ (%)	
theory, $\sigma_{th}$	0.10
acceptance	0.25
background	0.08
$e^\pm$ reconstruction	0.13
energy calibration	0.10
knowledge of $\sqrt{s}$	0.10
total: $\sigma_{th} \oplus \sigma_{exp}$	0.3

TABLE I: Relative systematic error on the luminosity measurement: experimental contributions are listed in detail and added in quadrature to yield the relative experimental error,  $\sigma_{exp}$ .

by 0.7% and the theoretical systematic uncertainty improved from 0.5% to 0.1%. The experimental uncertainty is summarized in Table I and is dominated by differences in the angular acceptance between data and MC.

#### V. EXTRACTION OF $a_\mu^{\pi\pi}$

The differential cross section is obtained from the observed spectrum,  $N_{obs}$ , after subtracting the residual background events,  $N_{bkg}$ , and correcting for the selection efficiency,  $\varepsilon_{sel}(M_{\pi\pi}^2)$ , and the luminosity:

$$\frac{d\sigma_{\pi\pi\gamma}}{dM_{\pi\pi}^2} = \frac{N_{obs} - N_{bkg}}{\Delta M_{\pi\pi}^2} \frac{1}{\varepsilon_{sel}(M_{\pi\pi}^2) \mathcal{L}}, \quad (2)$$

where our mass resolution allows us to have bins of width  $\Delta M_{\pi\pi}^2 = 0.01$  GeV<sup>2</sup>. The above formula is used in both small and large  $\gamma$  angle analyses.

The residual background content is found fitting the  $m_{trk}$  spectrum of the selected data sample with a superposition of Monte Carlo distributions describing the signal and background sources. The only free parameters of these fits are the relative weights of signal

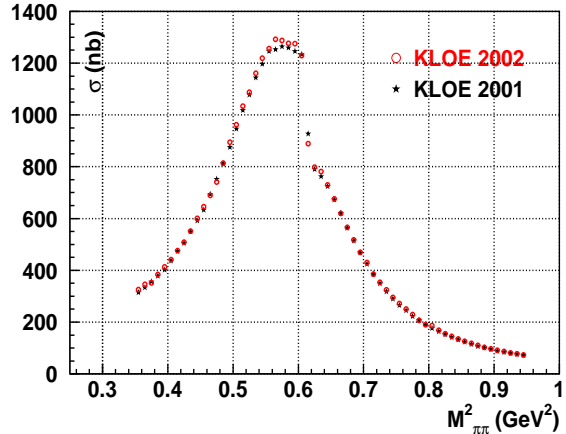


FIG. 2: Comparison between  $\sigma_{\pi\pi}$  measured in 2001 (dark star), updated for the trigger correction and for the new theoretical Bhabha cross section, and that measured in 2002 (light circle).

and backgrounds in data, computed as a function of  $M_{\pi\pi}$ .

The radiator function used to obtain  $\sigma_{\pi\pi}$  as in eq.(1) is provided by the code **Phokhara** [8], setting the pion form factor  $F_\pi(M_{\pi\pi}) = 1$ . In addition,  $\sigma_{\pi\pi}$  is corrected for the running of the fine structure constant [16] (vacuum polarization) and for shifting from  $M_{\pi\pi}$  to the virtual photon mass,  $M_{\gamma^*}$ , for those events with both an initial and a final photon. The **Phokhara** [9] version also having this contribution is used for the acceptance correction and for all efficiencies using the kinematics from Monte Carlo.

This corrected and FSR inclusive cross section,  $\sigma_{\pi\pi(\gamma)}^{bare}$ , is used to determine  $a_\mu^{\pi\pi}$ :

$$a_\mu^{\pi\pi} = \frac{1}{4\pi^3} \int_{s_{low}}^{s_{up}} ds \sigma_{\pi\pi(\gamma)}^{bare}(s) K(s), \quad (3)$$

where the lower and upper bounds of the spectrum measured with the small  $\gamma$  angle analysis are respectively  $s_{low} = 0.35$  GeV<sup>2</sup> and  $s_{up} = 0.95$  GeV<sup>2</sup>.

#### A. Comparison with the published result

Table II shows the list of relative systematic uncertainties in the evaluation of  $a_\mu^{\pi\pi}$  in the mass range [0.35,0.95] GeV<sup>2</sup>, for the published analysis of 2001 data and for the *preliminary* analysis of 2002 data. The comparison is performed for the same small  $\gamma$  angle selection.

In revisiting the published analysis we found a bias in the evaluation of the trigger correction that affects mostly the low  $M_{\pi\pi}$  region. Correcting for this effect and normalizing to the new Bhabha cross section we

systematic errors on $a_{\mu}^{\pi\pi}$ (%)		
	2001 analysis	2002 analysis
offline filter	0.6	negligible
background	0.3	0.3
kinematic cuts	0.2	0.2
$\pi/e$ ID	0.1	0.3
vertex	0.3	0.5
tracking	0.3	0.4
trigger	0.3	0.2
acceptance	0.3	0.1
FSR corrections	0.3	0.3
luminosity	0.6	0.3
$H$ function eq.(1)	0.5	0.5
vacuum polarization	0.2	negligible
total	1.3	1.1

TABLE II: Comparison of relative systematic errors on the extraction of  $a_{\mu}^{\pi\pi}$  in the mass range  $[0.35, 0.95]$   $\text{GeV}^2$  between the analysis of 2001 data and the *preliminary* analysis of 2002 data, using the same small  $\gamma$  angle selection.

updated the 2001 spectrum to compare with the new one from the 2002 analysis. Fig. 2 shows this comparison in terms of  $\sigma_{\pi\pi}$ .

$a_{\mu}^{\pi\pi}([0.35, 0.95] \text{ GeV}^2) \times 10^{10}$	
2001 published	$388.7 \pm 0.8_{stat} \pm 4.9_{sys}$
2001 updated	$384.4 \pm 0.8_{stat} \pm 4.9_{sys}$
2002 preliminary	$386.3 \pm 0.6_{stat} \pm 3.9_{sys}$

TABLE III: Comparison among  $a_{\mu}^{\pi\pi}$  values evaluated with the small  $\gamma$  angle selection.

The net shift is below one standard deviation on  $a_{\mu}^{\pi\pi}$ . Table III shows these results, which are in excellent agreement.

### B. Comparison between small and large $\gamma$ angle selections

An excellent cross check of the  $a_{\mu}^{\pi\pi}$  evaluation at small angle is from the measurement of  $\sigma_{\pi\pi}$  with photon emitted at large angle. Since it is an independent event selection scheme, that allows us also to test the knowledge of FSR contributions. Fig. 3 shows the comparison between the two spectra. In

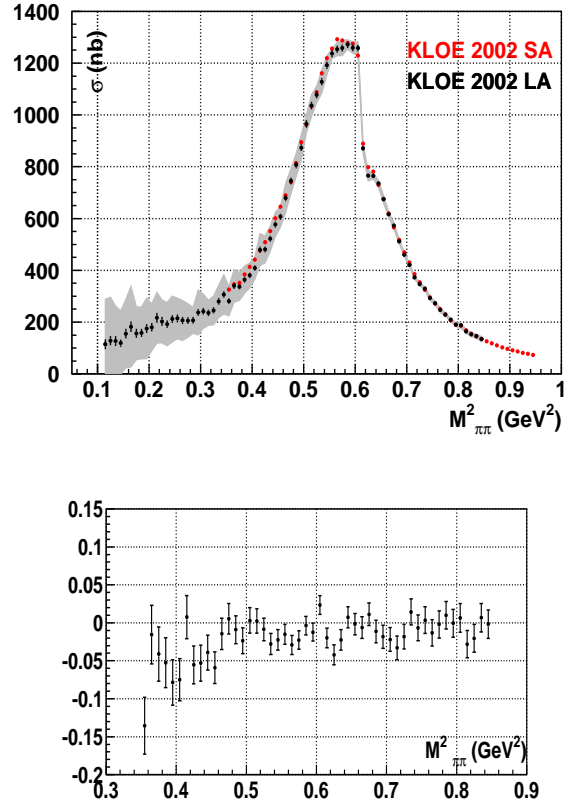


FIG. 3: Top: comparison between the small (SA) and large (LA)  $\gamma$  angle selections in  $\sigma_{\pi\pi}$ . In the latter case, also the systematic uncertainty is accounted for, as a band. Bottom: relative difference between the two cross sections shown in the upper panel.

the large angle case, the main source of uncertainty is the unknown interference between the FSR process and the resonant decays  $\phi \rightarrow \pi^+\pi^-\gamma$  – mentioned before – limiting the accuracy at low and high  $M_{\pi\pi}$  values, such that our comparison is limited to the range

$a_{\mu}^{\pi\pi}([0.5, 0.85] \text{ GeV}^2) \times 10^{10}$	
2002 small angle	$255.4 \pm 0.4_{stat} \pm 2.5_{sys}$
2002 large angle	$252.5 \pm 0.6_{stat} \pm 5.1_{sys}$

TABLE IV: Comparison between  $a_{\mu}^{\pi\pi}$  values evaluated with the small and large  $\gamma$  angle selections.

$[0.5, 0.85]$   $\text{GeV}^2$ . In that range we evaluated and compared  $a_{\mu}^{\pi\pi}$ . Table IV shows the good agreement for  $a_{\mu}^{\pi\pi}$  between the two independent measurements. The main source of systematic uncertainty in the large  $\gamma$  angle selection is from  $f_0(980)$  background subtraction.

### C. Preliminary comparison between KLOE and VEPP-2M experiments

We also made a comparison with the most recent  $a_\mu^{\pi\pi}$  evaluations released by the CMD-2 [17] and SND [18] experiments, in the mass range  $M_{\pi\pi} \in [630, 958]$  MeV. Table V shows this comparison, where

$a_\mu^{\pi\pi}(M_{\pi\pi} \in [630, 958] \text{ MeV}) \times 10^{10}$	
CMD-2 [17]	$361.5 \pm 1.7_{stat} \pm 2.9_{sys}$
SND [18]	$361.0 \pm 2.0_{stat} \pm 4.7_{sys}$
KLOE preliminary	$355.5 \pm 0.5_{stat} \pm 3.6_{sys}$

TABLE V: The  $a_\mu^{\pi\pi}$  value presented here compared with other recent evaluations.

the published CMD-2 and SND values agree with the new KLOE result within one standard deviation.

While the CMD-2 and SND dispersion integrals are performed with the trapezoid rule, the KLOE value is done extrapolating our bins to match the [630,958] MeV mass range, and summing directly the bin contents of the  $d\sigma_{\pi\pi\gamma}$  differential spectrum – weighed for the kernel function.

## VI. CONCLUSIONS AND OUTLOOK

We obtained the  $\pi\pi$  contribution to  $a_\mu$  in the mass range  $M_{\pi\pi}^2 \in [0.35, 0.95] \text{ GeV}^2$  integrating the differ-

ential cross section for the ISR events  $e^+e^- \rightarrow \pi^+\pi^-\gamma$ , measured with the KLOE detector:

1. the preliminary result from 2002 data agrees with the updated result from the published KLOE result, based on the small  $\gamma$  angle analysis of 2001 data;
2. the preliminary 2002 results both from the large and small  $\gamma$  angle analyses agree in a region where FSR effects play a minor role,  $M_{\pi\pi}^2 \in [0.5, 0.85] \text{ GeV}^2$ ;
3. the small angle 2002 result is also in agreement within one standard deviation with the recent SND and CMD-2 values in the mass range  $M_{\pi\pi} \in [630, 958] \text{ MeV}$ .

Further work is going on towards final results:

- refining the small angle analysis, *i.e.* by including the effects due to unfolding the detector resolution;
- improving the knowledge of the FSR interference effects for the large angle analysis, using KLOE  $f_0(980)$  measurements [10, 19];
- measuring the pion form factor directly from the ratio bin-by-bin of  $\pi^+\pi^-\gamma$  to  $\mu^+\mu^-\gamma$  spectra [20];
- extracting the pion form factor with a large angle selection from data taken at  $\sqrt{s} = 1 \text{ GeV}$ , off the  $\phi$  resonance.

- 
- [1] G. W. Bennett *et al.* [Muon G-2 Collaboration], Phys. Rev. D **73** (2006) 072003
- [2] F. Jegerlehner, “Essentials of the Muon g-2”, arXiv:hep-ph/0703125
- [3] M. Adinolfi *et al.*, [KLOE Collaboration] Nucl. Instrum. Meth. A **488** (2002) 51
- [4] M. Adinolfi *et al.*, [KLOE Collaboration] Nucl. Instrum. Meth. A **482** (2002) 364
- [5] S. Binner, J. H. Kühn and K. Melnikov, Phys. Lett. B **459** (1999) 279
- [6] A. Aloisio *et al.* [KLOE Collaboration], Phys. Lett. B **606** (2005) 12
- [7] A. Denig *et al.*, “Measurement of  $\sigma(e^+e^- \rightarrow \pi^+\pi^-\gamma)$  and extraction of  $\sigma(e^+e^- \rightarrow \pi^+\pi^-)$  below 1 GeV with the KLOE detector”, KLOE Note 192, July 2004, [www.lnf.infn.it/kloe/pub/knote/kn192.ps](http://www.lnf.infn.it/kloe/pub/knote/kn192.ps)
- [8] G. Rodrigo, H. Czyż, J. H. Kühn and M. Szopa, Eur. Phys. J. C **24** (2002) 71
- [9] H. Czyż, A. Grzelińska, J. H. Kühn and G. Rodrigo, Eur. Phys. J. C **47** (2006) 617
- [10] F. Ambrosino *et al.* [KLOE Collaboration], Phys. Lett. B **634** (2006) 148
- [11] H. Czyż, A. Grzelińska and J. H. Kühn, Phys. Lett. B **611** (2005) 116
- [12] G. Panzeri, O. Shekhovtsova and G. Venanzoni, Phys. Lett. B **642** (2006) 342
- [13] F. Ambrosino *et al.* [KLOE Collaboration], Eur. Phys. J. C **47** (2006) 589
- [14] C. M. Carloni Calame *et al.*, Nucl. Phys. B **584** (2000) 459
- [15] G. Balossini *et al.*, Nucl. Phys. B **758** (2006) 227
- [16] F. Jegerlehner, Nucl. Phys. Proc. Suppl. **162** (2006) 22
- [17] R. R. Akhmetshin *et al.* [CMD-2 Collaboration], Phys. Lett. B **648** (2007) 28
- [18] M. N. Achasov *et al.*, [SND Collaboration], J. Exp. Theor. Phys. **103** (2006) 380
- [19] F. Ambrosino *et al.* [KLOE Collaboration], Eur. Phys. J. C **49** (2007) 473
- [20] S. E. Müller and F. Nguyen *et al.* [KLOE Collaboration], Nucl. Phys. Proc. Suppl. **162** (2006) 90.